Research Article Vol. 3, No. 10 / 15 October 2020 / OSA Continuum 2880

Evaluation of mode division multiplexed system by dynamic power transfer matrix characterization

SMARANIKA SWAIN AND DEEPA VENKITESH*

Department of Electrical Engineering, Indian Institute of Technology Madras, Chennai - 600 036, India
**deepa@ee.iitm.ac.in*

Abstract: We experimentally demonstrate a simple method to characterize the temporal dynamics of the power transfer matrix of a mode division multiplexed (MDM) system using the time series of the output power in each channel. We consider a 3×3 MDM system consisting of a pair of 3-channel photonic lanterns (PL) for mode (de)multiplexing and 1 km of few-mode fiber (FMF) to evaluate the time evolution of channel selectivity, insertion loss, channel-dependent loss, and accumulated cross-talk for each channel. We further compare the statistics of time evolution of the above parameters for MDM systems utilizing mode-selective and non-mode-selective photonic lanterns. Such results are used to evaluate the consequences of choice of photonic lanterns and their utility in long-haul and short-reach mode division multiplexed systems.

1. Introduction

Continuous demand for bandwidth-hungry applications, supported by the steady increase in electronic processing speed, has paved the way for an exponential growth in capacity of fiber optic communication in the past few decades. Mode division multiplexing (MDM) using few-mode fiber (FMF) has emerged as a promising candidate for increasing transmission capacity [1]. Although the notion of using multimode fiber for optical communication dates as far back as 1982 [2], the recent progress in this field [3] is enabled by the phenomenal development in design and fabrication of few-mode fiber and components such as mode multiplexers and de-multiplexers (together referred to as (de)multiplexers in this paper), few-mode amplifiers, mode converters and mode add/drop multiplexers [4–7].

Spatial multiplexers are crucial components, properties of which play a critical role in converting the Gaussian transverse modes corresponding to that of the standard single-mode fibers to those compatible with the few-mode fibers. There are different types of spatial multiplexers available commercially, with specific advantages. Free-space based spatial multiplexers using phase plates or spatial light modulators render high mode extinction, but at the expense of bulky free-space setups and high coupling loss [8,9]. Photonic integrated circuits offer small device foot-print but with high coupling loss [10] due to low efficiency of coupling from fiber to waveguide. Photonic lanterns have recently become very popular as all-fiber mode coupling devices with tolerable insertion loss and a reasonable reliability. A photonic lantern (PL) is an $N \times 1$ all-fiber mode multiplexer, in which N single-mode fibers (SMFs) are adiabatically tapered into a single larger core corresponding to that of a few-mode fiber. The adiabatic transition results in a unitary transformation of the N independent signals from the SMFs to N specific modes or a combination of modes in the FMF.

In an $N \times N$ MDM system employing photonic lanterns as mode (de)multiplexers, N optical transmitters are used as input to the $N \times 1$ input PL followed by the FMF and the $1 \times N$ output PL, the N outputs of which are applied to the N independent receivers. The capacity of an ideal $N \times N$ MDM system increases proportionally with the number of propagating modes (N) [3]. However, a practical MDM system is limited by the mode-dependent impairments such

#398754 https://doi.org/10.1364/OSAC.398754
Journal © 2020 Received 1 Jun 2020; revised 1 Oct 2020; accepted 1 Oct 2020; published 13 Oct 2020

OSA CONTINUUM

as mode-dependent loss, cross-talk, and differential modal group delay, which also decide the digital signal processing (DSP) complexity. The differences in the group velocities between the modes of an MDM system, characterized by the differential modal group delay (DMGD), is an important parameter that decides the complexity of the digital signal processing at the receiver. The DMGD of the FMF used in our experiment is measured to be 60 ps/km using a Fourier domain mode locked laser [11]. Characterization of DMGD and knowledge of the transmission matrix of the PL-FMF-PL system is essential to understand the channel dynamics and optimize the system performance.

Space division multiplexed-optical vector network analyzer (SDM-OVNA) based on swept wavelength interferometry provides a quantitative estimation of complex transfer matrix across a desired range of wavelength [12]. Measurement of mode-coupling in FMF is reported in [13] and [14] using impulse response (IR) measurement and spatially and spectrally resolved (S^2) imaging technique respectively. While the complexity in hardware requirements in these methods are relatively smaller, they characterize only the mode-coupling in the fiber and hence provide only partial information on the linear transfer characteristics of the MDM system. There also have been few demonstrations based on back-scattered power in an FMF, which measure only the mode-coupling strength [15,16]. The Brillouin optical time-domain reflectometer [16] is also limited by measurement distance due to reduction in stimulated Brillouin scattering efficiency [16]. Although there have been several methods reported to characterize the mode-dependent properties, estimation of the complex linear transfer matrix is the most comprehensive approach, since it gives a very clear understanding of the mode-dependent properties of the $N \times N$ transfer matrix. The measurement technique based on Rayleigh backscattering amplitudes [17] is simple, but involves the use of an FMF circulator. A similar technique based on optical reflection reported in [18] characterizes the power transfer matrix by using a highly reflective mirror at the end of the FMF which allows the collection of back-propagated signal in the input PL. Hence, it does not characterize the transfer matrix of a practical PL-FMF-PL system in which the input and output PLs are actually different. Mode coupling dynamics in FMF has been studied in [19,20] by estimating the complex field at faster time scales. However, this approach for characterization of MDM systems involves complex expensive hardware while being energy-consuming. Study of the temporal dynamics of the MDM system using a simplified approach is practically useful. The crosstalk dynamics of an SDM system using few-mode multi-core fiber is investigated in [21] by launching different wavelengths in different modes and by capturing the outputs sequentially from each core, in an optical spectrum analyzer. In this study, we perform a simultaneous measurement of all the output modes, while using a common wavelength of operation for all the spatial modes. In addition to communication systems, FMFs find a wide range of applications in sensing, microwave photonics and in optical signal processing [22–25]. The characterization technique presented here would be useful in such applications as well.

In this work, we experimentally demonstrate a simple, on-the-fly, and non-destructive power transfer matrix characterization technique using minimal hardware. We evaluate channel selectivity, insertion loss, channel-dependent loss and coupling strength of the PL-FMF-PL system in both forward and reverse directions. We also study the time evolution of these properties to understand the channel dynamics and compare the results for mode-selective and non-mode-selective excitation. We use the statistical understanding of the mode-dependent properties to comment on the relevance of mode excitation method on system performance both for short-reach and long-haul systems. In Section 2, we define different performance metrics of an MDM system and discuss their relevance. In Section 3 we discuss the experimental setup to measure these parameters and in Section 4 we discuss the details of the experimental results along with their relevance in an MDM system.

OSA CONTINUUM

2. Theory

An $N \times N$ PL-FMF-PL system is characterized by the power transfer matrix,

$$T = [R_{ij}]; \qquad 1 \leq i,j \leq N \tag{1}$$

where R_{ij} is the excitation efficiency which represents the fraction of power input in a particular channel (i) of the input PL (P_i^{in}) that gets coupled in a particular channel (j) of the output PL (P_j^{out}). R_{ij} is mathematically defined as $R_{ij} = \frac{P_j^{out}}{P_i^{in}}$. Figure 1 schematically represents the excitation efficiencies for a 3×3 PL-FMF-PL system. Each column of T contains the excitation efficiencies corresponding to a particular input channel of the PL-FMF-PL system.

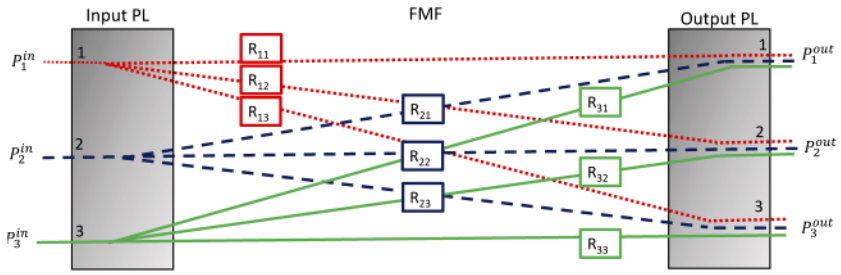

Fig. 1. Schematic representing the excitation efficiencies (R_{ij} $i,j = 1,2,3$) in a PL-FMF-PL system

There are broadly two types of photonic lantern designs based on their excitation properties namely (a) non-mode-selective photonic lantern and (b) mode-selective photonic lantern. In a non-mode-selective photonic lantern (NMPL), N SMFs of identical core diameters are adiabatically merged to excite an orthogonal combination of modes supported in the FMF [26]. A mode-selective photonic lantern (MPL) on the other hand, excites only specific modes from a given input SMF. This design was first proposed in [27], where N independent pre-tapered SMFs of dissimilar core diameters are adiabatically combined in order to achieve selective excitation of modes. Mode-selectivity in a photonic lantern requires breaking the degeneracy between the modes while avoiding any overlap between the propagation constants during the transition.

In case of an ideal PL-FMF-PL system consisting of reciprocal and identical PLs used as multiplexer and demultiplexer, T is expected to be an identity matrix which means, power launched in channel i of input PL is expected to get coupled to only channel i of the output PL. However, in a practical scenario, photonic lanterns have finite mode extinction, the input signal experiences mode-dependent propagation effects in the FMF such as differential modal group delay, intermodal mixing, and mode-dependent loss and no two fabricated lanterns (used for multiplexing and demultiplexing) have identical transfer functions. Characterization of an individual PL and/or FMF contributes to the understanding of the MDM system, albeit partially. The output of an MDM system is not only affected by the power coupling between modes but also by the nature of mode (de)excitation at the input and output of FMF. The mismatch between the PLs and the FMF under test, would also influence the coupling matrices. Hence, it is important to characterize the complete PL-FMF-PL system.

The individual SMF ports of the input PL are used to launch signal with Gaussian transverse intensity profile in an MDM system. Based on the design of the multiplexer used (MPL or NMPL), signal launched in a particular port of the input PL excites either a specific mode or a combination of modes in the FMF-end of the PL. Similarly, after propagation in the FMF, based on the design of the demultiplexer used, either signal corresponding to a specific mode or signal corresponding to a linear combination of the supported modes is recovered in the individual SMF ports of the

OSA CONTINUUM

output PL. Each pair of input-output port in the $N \times N$ PL-FMF-PL system is considered as an information carrying channel. Since we consider both mode-selective and non-mode-selective photonic lanterns in this work, we will use the term "channel" instead of "mode" to define the properties of the MDM system [18]. If we use a pair of ideal mode-selective PLs in the back-to-back configuration, "channel" is identical to "mode", while in case of non-mode-selective PLs, "channel" would refer to a combination of modes.

A practical PL-FMF-PL system can then be characterized using the following channel-dependent metrics : (a) channel selectivity (CS), (b) insertion loss (IL), (c) channel-dependent loss (CDL), and (d) cross-talk based on the excitation efficiencies [18]. These properties are used to characterize each channel of a PL-FMF-PL system by assuming, power is launched only in that channel of the input PL. The mathematical definitions of the above-mentioned properties are stated in Table 1. Channel selectivity in linear scale is defined as the ratio of the diagonal excitation efficiency (R_{ii}) to the summation of the non-diagonal excitation efficiencies of the i^{th} column, and it quantifies the power leaked into other channels. Larger the selectivity, smaller is the leakage of power to other channels. On the other hand, insertion loss of channel i in linear scale is defined as the sum of all the excitation efficiencies in i^{th} column of the power transfer matrix. Channel-dependent loss of a given channel is measured relative to the channel with the least insertion loss. It is the difference (in logarithmic scale) in insertion loss experienced by a channel compared to the minimum insertion loss observed in the system.

Table 1. Channel-dependent metrics of the PL-FMF-PL system. P_i^{out}, P_j^{out} : power in the i^{th}, j^{th} output channels respectively.

Property	Mathematical representation
Channel selectivity	$CS_i = 10\log_{10}\left(\frac{R_{ii}}{\sum_j R_{ij}}\right), j \neq i$
Insertion loss	$IL_i = -10\log_{10}\left(\sum_j R_{ij}\right)$
Channel-dependent loss	$CDL_i = IL_i - min(IL_i)$
Accumulated cross-talk	$XT_i = 10log_{10}\left(\frac{\sum_j P_j^{out}}{P_i^{out}}\right) = -CS_i \; ; j \neq i$

Signal launched in a particular mode of FMF can get coupled to a different mode during propagation due to non-uniform index distribution and/or longitudinal variation of fiber geometry along the length of FMF. Coupling strength or accumulated cross-talk in channel i denoted as XT_i, is also defined under the condition of single channel launch [28] at the input. It is the ratio of total power in all the other channels after propagation through the PL-FMF-PL system to power remaining in the launching channel [28]. It is important to notice that cross-talk and channel selectivity are negative of each other in logarithmic scale. Large value of coupling strength suggests considerable leakage of power from the launched channel to the other channels. In order to achieve theoretically expected capacity, it is desired to have maximum channel selectivity and minimum insertion loss in each channel. Absence of channel-dependent loss is also desirable such that each MDM channel equally contributes to the expected increase in channel capacity. We now proceed to experimentally characterise the PL-FMF-PL system using the above metrics.

3. Experimental setup

We consider a 3×3 PL-FMF-PL system where 1 km long three-mode graded-index fiber supporting LP_{01}, LP_{11a} and LP_{11b} modes is spliced on both ends to a pair of commercially procured photonic lanterns. The choice of this length is based only on the availability of the

OSA CONTINUUM

fiber. However, the proposed technique can be applied to characterize a PL-FMF-PL system consisting of any length of FMF. We study the channel-dependent properties and the linear transfer characteristics of the following two PL-FMF-PL systems.

1. NMPL1 - 1 km FMF - NMPL2 with non-mode-selective (de)multiplexer
2. MPL1 - 1 km FMF - MPL2 with mode-selective (de)multiplexer

The schematic of the experimental setup is shown in Fig. 2(a). Output of laser source at 1550 nm (linewidth 2 MHz) with 6.25 dBm average power is connected to each channel of the input PL, one at a time. Note that the definition of R_{ij} defined in Section 2 requires a single-channel launch condition. The images obtained from an infrared charge-coupled camera device, captured at the FMF side of NMPL1 and MPL1, when each channel is excited individually is shown in Fig. 2(b). Note that images shown in Fig. 2(b) are not at the output of the PL-FMF-PL system, but at the output of the input PL. Outputs of the PL-FMF-PL system are SMFs and hence the corresponding outputs are expected to have Gaussian profiles. The application of signal to an individual input SMF of NMPL excites a distinct linear combination of the supported modes in the FMF end whereas the MPL excites specific modes at the FMF end based on the input channel excited. It is to be noted here that, as shown in Fig. 2(b), channel 2 of the NMPL1 excites significant fundamental mode content compared to the other channels.

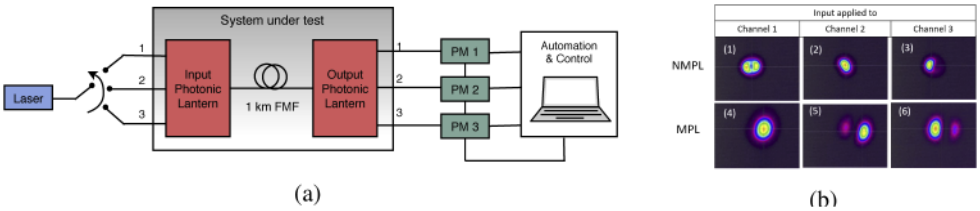

Fig. 2. (a) Schematic of the experimental setup; PM: power meter and (b) Images at the FMF end when input being applied to each channel of NMPL1 (1-3) and MPL1 (4-6)

The input PL is spliced to a 1 km long graded-index few-mode fiber (OFS-60815), which is further spliced to the FMF-end of the output PL. Core matching with a commercial arc-fusion splicer is used in the automated mode, and this ensures minimal splice loss [29]. The PLs are fabricated such that the FMF used in the PL and that used in the transmission fiber match in their refractive index profiles and numerical aperture. Power at the three ports of the output PL are monitored simultaneously using three power meters (represented as PM1, PM2 and PM3 in Fig. 2(a)), and the data acquisition is automated and controlled with a computer, with a capture rate of 5 samples/second and a total duration of 30 minutes. The data acquisition from all the three power meters are synchronised so that the power received in all the three output ports are logged simultaneously. The automated process is repeated by launching power in each channel of the input PL. The recorded time series are used to evaluate the parameters discussed in Section 2. The experiments are repeated with both NMPL and MPL. Reciprocity of the transmission system is verified by launching power from the output end and recording the power at the input end of the setup shown in Fig. 2(a). Experiments are also repeated without the FMF by directly splicing the two PLs in order to study the influence of FMF on the channel transfer matrix and its time dynamics.

4. Results and discussion

After propagation through FMF and the output PL, power in each output channel is expected to be a linear combination of the power excited in the input channels. However, weights of the excited

OSA CONTINUUM

modes fluctuate with time due to environmental disturbances and this leads to a time-varying transfer of power from one channel to the other. We proceed to evaluate the time evolution of the excitation efficiencies from the recorded time series captured using PM1, PM2 and PM3. We further evaluate the time evolution of channel-dependent properties mentioned in Table 1 using excitation efficiencies defined in Eq. 1. We plot histograms corresponding to the time series of channel selectivity, insertion loss and channel-dependent loss of the PL-FMF-PL systems for an observation duration of 30 minutes. We discuss below the inferences drawn on each of the channel-dependent properties.

4.1. Channel selectivity

The time series showing channel selectivity of each channel of the MPL-FMF-MPL and the NMPL-FMF-NMPL system are shown in Fig. 3(a). In case of the MPL-FMF-MPL system, channel 1 which excites fundamental mode in the FMF has the highest selectivity (mean: 7.27 dB). However, in case of the NMPL-FMF-NMPL system, channel 2 has the highest selectivity (mean: 2.07 dB). As discussed in Section 3 and shown in Fig. 2(b), signal excited by channel 2 of NMPL1 has strong fundamental mode content. The coupling strength of a particular channel is the inverse of its channel selectivity as discussed in Section 2. Hence, from Fig. 3(b), it can be deduced that channel 2 in case of the NMPL-FMF-NMPL system and channel 1 in case of MPL-FMF-MPL system have the least coupling strength (less prone to coupling). Fundamental LP_{01} mode is excited predominantly by channel 1 and 2 of the MPL and NMPL respectively. Hence, it can be inferred that the fundamental mode is less prone to coupling and is excited with the highest selectivity irrespective of the design of photonic lantern. The design of the photonic lantern plays a major role in preserving the purity of the fundamental mode. However, the specific mode pattern of the fundamental mode where the energy is confined to the center of the fiber makes it more resistant to the impact of mode coupling [21,28].

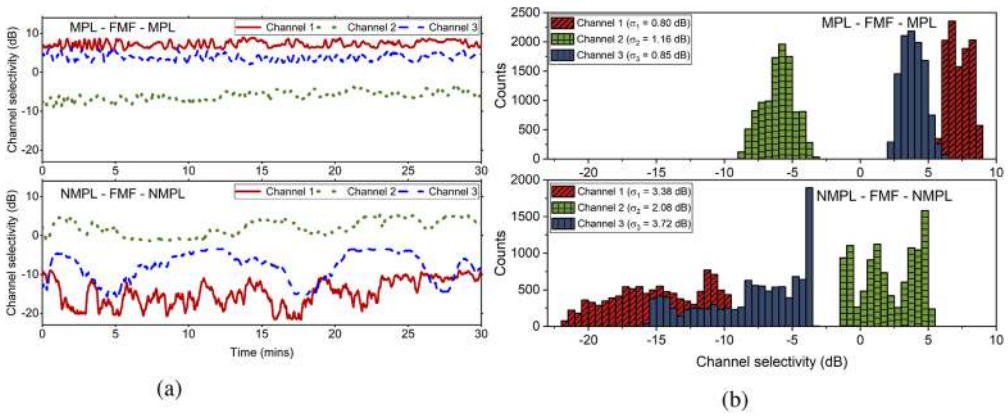

Fig. 3. (a) Time series and (b) histograms representing variation of CS of all the channels in case of MPL-FMF-MPL and NMPL-FMF-NMPL system for a duration of 30 minutes

Histograms showing variation in channel selectivity of each channel of the two PL-FMF-PL systems are shown in Fig. 3(b) with the standard deviation observed in these parameters mentioned in the inset. For a duration of 30 minutes, channel selectivities of all the three channels are found to fluctuate with considerably larger variances in case of the NMPL-FMF-NMPL system compared to that observed in case of the MPL-FMF-MPL system as evident from the spread of the histograms in both cases. This clearly shows that, for the given length of FMF, channel conditions are more stable for mode-selective excitation compared to non-mode-selective excitation. There is also considerable overlap observed among the histograms of channels 1 and

OSA CONTINUUM

3 in case of the NMPL-FMF-NMPL system whereas there is hardly any overlap between the histograms in the MPL-FMF-MPL system. This indicates that channel selectivity has strong mode dependence and is hence distinctly different for various channels of the MPL-FMF-MPL system. This also explains the distinct selectivity of channel 2 of the NMPL-FMF-NMPL system which has strong fundamental mode content. The larger spread and overlap in the histograms of the NMPL-FMF-NMPL system also indicate continuous transfer of power between channels and hence stronger coupling compared to the MPL-FMF-MPL system for the same length of FMF.

Interplay of cross-talk between channels and differential modal group delay deteriorates transmission distance and performance thus playing a critical role in deciding the capacity and digital signal processing complexity of an MDM system [30,31]. There are two general approaches to reduce computational complexity and resulting energy consumption per bit of a multi-input-multi-output (MIMO) equalizer. The first approach, more suitable for a long-haul link, is to use strong coupling such that each mode is statistically fully coupled with other modes resulting in reduction of group delay spread. The second approach which is more applicable for a short-haul MDM system is to have limited coupling strength along the length of the fiber (high mean and low standard deviation of channel selectivities). The relatively high channel selectivities observed in case of the MPL-FMF-MPL system is desirable for short-haul optical links which require low-cost implementation and hence minimal DSP. However, for long-haul optical links, where mode coupling is inevitable, non-mode-selective (de)excitation is more suitable. In such a case, significantly different channel selectivity in a particular channel (as observed in channel 2 of the NMPL-FMF-NMPL system in our case) can lead to unequal convergence time for different channels of the MDM system. Hence, it is desirable to have better accuracy in fabrication of PLs to avoid mode-selectivity in any particular port of a non-mode-selective PL. The quantification of channel-dependent properties using the power transfer matrix approach is a simple method to evaluate the system performance by identifying the relative coupling strength of different channels in an MDM system.

4.2. Insertion loss

The time series and histograms showing variation in insertion loss of each channel of the MPL-FMF-MPL and NMPL-FMF-NMPL systems are shown in Fig. 4(a) and Fig. 4(b) respectively for an observation duration of 30 minutes. The maximum insertion loss per photonic lantern as per the test reports is $\approx$ 3.5 dB. Hence, the worst-case overall loss for the PL-FMF-PL system is expected to be $\approx$ 8 dB, considering an insertion loss of $\approx$ 1 dB for the 1 km long FMF and the splice losses. However, average value of the experimentally observed insertion loss shown in Fig. 4(b) is found to be higher in the case of MPL, especially for the higher-order modes, possibly because of the non-ideal polarisation state of the mode launched into the output lantern. The performance of the MPL is expected to be dependent on the input polarisation conditions [18]. Electronic control of input polarisation state may further improve the insertion loss values of the input lantern, but since the FMF is non-polarisation maintaining, the polarization state of the launched power into the output lantern may not be ideal, resulting in a larger overall loss- as observed in the manuscript. This would be the scenario in a practical communication link as well. In the case of NMPL, the average of the measured loss values match with those in the test reports.

Channel 1 of the MPL-FMF-MPL system has the least insertion loss and channel 3 has the highest insertion loss. In case of NMPL-FMF-NMPL system, the insertion loss of the three channels are mostly identical. However, channel 2 (with predominant fundamental mode excitation) has the least insertion loss among all channels. It is important to note here that low channel selectivity does not necessarily mean high insertion loss and vice versa as evident from Fig. 3 and Fig. 4. This is because low CS implies relatively smaller magnitude of $\sum R_{ij}$ $(i \neq j)$ compared to R_{ii} whereas insertion loss represents $\sum_j R_{ij}$ which is independent of their relative magnitudes. There is very limited fluctuation in IL recorded in both cases over the observation

OSA CONTINUUM

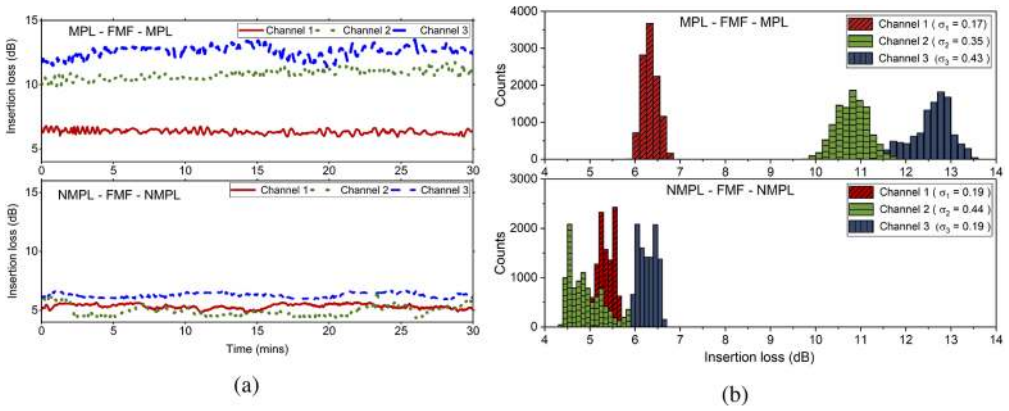

Fig. 4. (a) Time series and (b) histograms showing the variation of IL in case of MPL-FMF-MPL and NMPL-FMF-NMPL system for a duration of 30 minutes

duration of 30 minutes as indicated by the small values of standard deviation in each case. The FMF considered in this work exhibits negligible insertion loss of around 0.2 dB/km similar to that observed in standard single-mode fiber. Hence, the insertion loss of a PL-FMF-PL system is largely contributed by the pair of photonic lanterns used for (de)multiplexing, especially for short-haul links. Even though low insertion loss is the most remarkable feature of all-fibre photonic lanterns compared to other (de)multiplexing technologies, the insertion loss observed in a particular channel of a commercial PL depends on the excited mode and the accuracy of the tapering and fusion process. The significantly higher insertion losses observed in channels 2 and 3 of the MPL-FMF-MPL system compared to the NMPL-FMF-NMPL system indicate that higher order modes are more susceptible to minor imperfections in the fabrication process leading to higher levels of loss. Unequal insertion loss of channels leads to disparity in signal-to-noise ratio and departure from the mode orthogonality in the receiver.

4.3. Channel-dependent loss

As discussed in Section 4.2, channels 1 and 2 experience the least insertion loss in case of the MPL-FMF-MPL and the NMPL-FMF-NMPL system respectively and hence are used as reference channels for the channel-dependent loss calculations. The time series and histograms showing variation of channel-dependent loss in case of MPL-FMF-MPL system (for channels 2 and 3) and NMPL-FMF-NMPL system (for channels 1 and 3) are shown in Fig. 5(a) and Fig. 5(b) respectively for an observation duration of 30 minutes. Histograms showing the variation in CDL of channels 2 and 3 for the MPL-FMF-MPL system and of channels 1 and 3 for the NMPL-FMF-NMPL system are shown in Fig. 5(b). Channel-dependent loss of the NMPL-FMF-NMPL system is significantly lower compared to the MPL-FMF-MPL system. This is because, as discussed in Section 4.2, the insertion loss of different channels of the NMPL-FMF-NMPL system are mostly identical and hence difference in insertion losses are significantly low. Similar to IL, there is very limited fluctuation observed in the time series data as evident from standard deviation values mentioned as inset of Fig. 5(b). Chcannel-dependent loss has very detrimental impact on the complexity and performance of an MDM system. The presence of a strong channel experiencing low insertion loss results in the issue of singularity in the MIMO DSP of an MDM system where all the weaker data tributaries converge to the stronger channel [32].

The presence of large channel-dependent loss represents the non-unitary nature of the MDM power transfer matrix. Mode multiplexers and few-mode amplifiers are generally found to

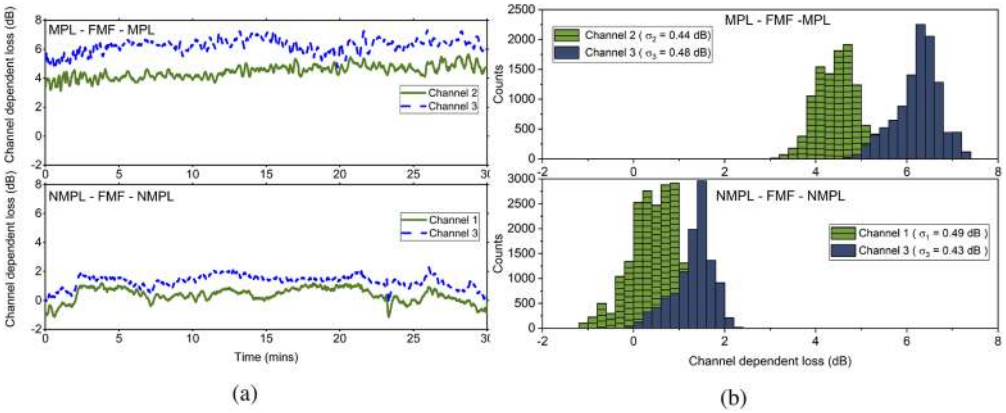

Fig. 5. (a) Time series and (b) histograms showing the variation of CDL of all the channels in case of MPL-FMF-MPL and NMPL-FMF-NMPL system for a duration of 30 minutes.

contribute to the mode-dependent loss. Hence, even though the results shown in this work are for FMF of length 1 km, the inference of the MPL-FMF-MPL system being significantly more non-unitary compared to a NMPL-FMF-NMPL system is expected to be true for longer lengths of FMF as well. Appropriate pre-equalization of input power or modified MIMO DSP routines are essential in combating the CDL-induced singularity issue in MDM application [32].

4.4. Reciprocity of Power Transfer Matrix

In order to verify the reciprocity of the system, experiments are repeated by launching power from the output end as shown in Fig. 2(a), and the received power is observed in different ports at the input end. In case of the NMPL-FMF-NMPL system, the mean channel selectivity of all three channels are comparable in the reverse operating condition whereas the values are significantly different in the forward operating condition. The maximum observed variance in channel selectivity is > 10 dB for two channels of the NMPL-FMF-NMPL system in the forward condition whereas the overall fluctuation is comparatively lower in the reverse direction of operation. Under stable laboratory conditions, we do not expect the channel conditions to drastically differ in the forward and reverse direction of operation. Hence, it can be inferred that the PL-FMF-PL system is not reciprocal in terms of mode coupling and the input PL plays a significant role in deciding the stability (low variance of CS) of the power transfer matrix, especially for short-haul MDM links. For a given length of FMF, a slow variation in channel selectivity and hence coupling strength results in less frequent filter tap update. Hence, the stability in the power transfer matrix is always desirable and the choice of input PL is critical. However, the difference in performance between forward and reverse operating conditions is not observed in case of insertion loss and channel-dependent loss. This is because, unlike CS, these two properties represent end-to-end loss and hence do not depend on input condition.

The magnitudes of the normalised power transfer matrices of the MPL-FMF-MPL and the NMPL-FMF-NMPL systems are visually represented in Fig. 6(a) and Fig. 6(b) under forward and reverse operating conditions respectively, where the gray scale represents the strength of the respective excitation efficiency. These are evaluated using the mean excitation efficiencies calculated from the time series data. A PL-FMF-PL system is expected to transmit all the channels with equal and high selectivity at low insertion loss in the presence of unitary mode mixing (CDL = 0 dB) to achieve optimal performance, longer reach and minimal DSP complexity. We found that the channel-dependent properties in a practical PL-FMF-PL system vary with the design of mode (de)multiplexer, specifically with the choice of input multiplexer. The non-unitary

OSA CONTINUUM

nature of the MPL-FMF-MPL system is evident in both forward and reverse operating conditions with significantly higher value of R_{11} compared to R_{12} and R_{13}. Similarly, channel 2 in case of NMPL-FMF-NMPL system has higher selectivity compared to the other channels (R_{22}>R_{21}, R_{23}). However, the NMPL-FMF-NMPL system has a better distribution of power in different channels compared to the MPL-FMF-MPL system.

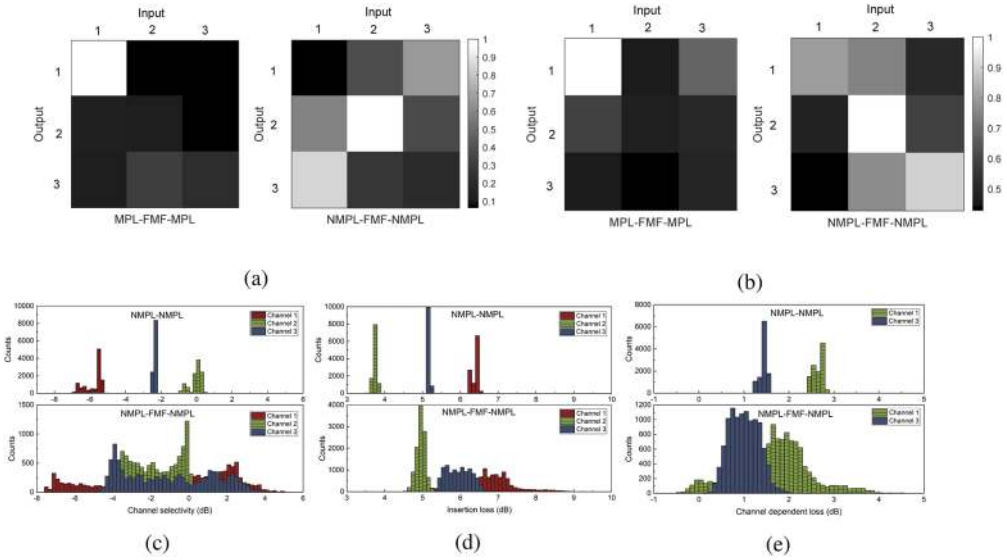

Fig. 6. Power transfer matrices for MPL-FMF-MPL and NMPL-FMF-NMPL system in (a) forward and (b) reverse operating condition. Histograms showing variation of (c) channel selectivity, (d) insertion loss, and (e) channel-dependent loss in case of non-mode-selective (de)excitation for a duration of 30 minutes in back-to-back condition and in the presence of FMF.

Fluctuation in channel selectivity is much higher in case of the NMPL-FMF-NMPL system (larger variance value) as shown in Fig. 3 indicating more frequent transfer of power among channels. Usage of mode-selective photonic lantern for excitation can result in high channel-dependent loss while minimizing mode coupling at the multiplexers. However, usage of non-mode-selective lantern can potentially induce intermodal coupling in the presence of minimal channel-dependent loss. Strong intermodal coupling is reported to reduce the group delay spread [30]. Hence, in case of long-haul MDM links, where presence of CDL can be extremely detrimental on the DSP, a non-mode-selective excitation can be useful since intermodal coupling is anyway inevitable in the FMF beyond 100s of km. However, for short-haul applications where mode-coupling in FMF is limited to weak polarization-coupling, usage of mode-selective lantern may be useful to limit the accumulated cross-talk and hence DSP complexity.

4.5. Influence of FMF

We now proceed to evaluate the role of FMF in our observed results. The histograms corresponding to channel selectivity, insertion loss and channel-dependent loss are shown in Fig. 6(c), 6(d) and 6(e) respectively for the case of non-mode-selective excitation in back-to-back condition and in the presence of 1 km FMF, for the reverse operating condition. It is clear that variance of the parameters are considerably increased in the presence of FMF. This is expected since there is transfer of power between the channels due to the presence of coupling events resulting from environmental perturbations and imperfections in index and uniformity of core, cladding along the length of FMF. The minimal variance in the channel properties in back-to-back condition for

OSA CONTINUUM

the same observation duration confirms that the variance observed in the presence of FMF has limited dependence on interference due to change in center frequency fluctuations of input signal. As discussed in Section 2, for a given length of FMF, the accumulated cross-talk of a channel is inversely proportional to the channel selectivity. Knowledge of accumulated cross-talk in both back-to-back condition and in the presence of FMF, can aid in characterizing the distribution of perturbation due to the length of FMF [28].

The mode mismatch between the PLs and that between the PLs and the FMF can lead to potential error in simultaneous characterization of different channels of the FMF. This inevitable mismatch could be compensated by use of a tunable mode coupler system placed at transition points from SMF to FMF and vice versa [33,34]. In-situ modal decomposition could be used to adjust pressure applied on the FMF placed below a micro-bending based long period fiber grating (LPFG) [35]. After achieving the best possible mode matching between the PLs and the FMF, the procedure mentioned in this work can be followed to obtain more accurate information about the mode coupling effects of the few-mode fiber.

5. Conclusion

We present a simple power-transfer matrix characterization method for an MDM system and experimentally demonstrate the same for an all-fiber 3×3 system involving a 1-km long few-mode graded-index fiber with photonic lanterns used for mode (de)excitation. We evaluate the time evolution of channel selectivity, insertion loss and channel-dependent loss for each channel of two systems using (a) mode-selective excitation and (b) non-mode-selective excitation. Fundamental mode is found to be excited with the highest selectivity irrespective of the design of photonic lantern. We find that the PL-FMF-PL system is not necessarily a reciprocal system and the choice of a specific configuration has implications on the stability and performance of the overall system. Mode-selective excitation is found to induce large channel-dependent loss in the presence of slow time variation of channel-dependent properties while non-mode-selective excitation is found to induce a fast variation of channel-dependent properties with negligible channel-dependent loss. Digital equalization of system and channel impairments in an MDM system involves computationally complex multi-input multi-output signal processing which scales linearly with the number of propagating channels and group delay spread. Hence, simple and energy efficient on-the-fly characterization techniques are essential in understanding the system dynamics, which helps in accurate channel modelling and appropriate optimization of input conditions to improve performance. Although in this work we considered an all-fiber MDM system involving 1-km of FMF, the proposed technique is useful in end-to-end characterization of a complete MDM system using any alternate mode multiplexer, longer length of FMF or in the presence of any other few-mode component in the link such as few-mode amplifier or mode add-drop multiplexer.

Funding

Indian Institute of Technology Madras(EE1920250RFTP008428); Ministry of Electronics and Information technology (No. 1(10)2016-EMCD); Visvesvaraya PhD scheme (MEITY-PHD-2692).

Disclosures

The authors declare no conflicts of interest.

References

1. G. Li, N. Bai, N. Zhao, and C. Xia, "Space-division multiplexing: the next frontier in optical communication," Adv. Opt. Photonics **6**(4), 413–487 (2014).
2. S. Berdagué and P. Facq, "Mode division multiplexing in optical fibers," Appl. Opt. **21**(11), 1950–1955 (1982).

OSA CONTINUUM

3. G. Rademacher, R. S. Luís, B. J. Puttnam, T. A. Eriksson, R. Ryf, E. Agrell, R. Maruyama, K. Aikawa, Y. Awaji, H. Furukawa, and N. Wada, "High capacity transmission with few-mode fibers," J. Lightwave Technol. **37**(2), 425–432 (2019).
4. L. Grüner-Nielsen, Y. Sun, J. W. Nicholson, D. Jakobsen, K. G. Jespersen, J. Robert Lingle, and B. Pálsdóttir, "Few mode transmission fiber with low dgd, low mode coupling, and low loss," J. Lightwave Technol. **30**(23), 3693–3698 (2012).
5. N. Bai, E. Ip, Y.-K. Huang, E. Mateo, F. Yaman, M.-J. Li, S. Bickham, S. Ten, J. Li nares, C. Montero, V. Moreno, X. Prieto, V. Tse, K. M. Chung, A. P. T. Lau, H.-Y. Tam, C. Lu, Y. Luo, G.-D. Peng, G. Li, and T. Wang, "Mode-division multiplexed transmission with inline few-mode fiber amplifier," Opt. Express **20**(3), 2668–2680 (2012).
6. Y. Zhao, Y. Liu, C. Zhang, L. Zhang, G. Zheng, C. Mou, J. Wen, and T. Wang, "All-fiber mode converter based on long-period fiber gratings written in few-mode fiber," Opt. Lett. **42**(22), 4708–4711 (2017).
7. T. A. Birks, I. Gris-Sánchez, S. Yerolatsitis, S. G. Leon-Saval, and R. R. Thomson, "The photonic lantern," Adv. Opt. Photonics **7**(2), 107–167 (2015).
8. R. E. Freund, C. Bunge, N. N. Ledentsov, D. Molin, and C. Caspar, "High-speed transmission in multimode fibers," J. Lightwave Technol. **28**(4), 569–586 (2010).
9. R. Ryf, S. Randel, A. H. Gnauck, C. Bolle, A. Sierra, S. Mumtaz, M. Esmaeelpour, E. C. Burrows, R.-J. Essiambre, P. J. Winzer, D. W. Peckham, A. H. McCurdy, and R. Lingle, "Mode-division multiplexing over 96 km of few-mode fiber using coherent 6×6 mimo processing," J. Lightwave Technol. **30**(4), 521–531 (2012).
10. N. K. Fontaine, C. R. Doerr, M. A. Mestre, R. R. Ryf, P. J. Winzer, L. L. Buhl, Y. Sun, X. Jiang, and R. Lingle, "Space-division multiplexing and all-optical mimo demultiplexing using a photonic integrated circuit," in *OFC/NFOEC*, (2012), pp. 1–3.
11. V. Kelkar, S. Swain, and D. Venkitesh, "Measurement of differential modal group delay of a few-mode fiber using a fourier domain mode-locked laser," Opt. Lett. **43**(9), 2165–2168 (2018).
12. N. K. Fontaine, R. Ryf, M. A. Mestre, B. Guan, X. Palou, S. Randel, Y. Sun, L. Grüner-Nielsen, R. V. Jensen, and R. Lingle, "Characterization of space-division multiplexing systems using a swept-wavelength interferometer," in *2013 Optical Fiber Communication Conference and Exposition and the National Fiber Optic Engineers Conference (OFC/NFOEC)*, (2013), pp. 1–3.
13. R. Maruyama, N. Kuwaki, S. Matsuo, and M. Ohashi, "Relationship between mode coupling and fiber characteristics in few-mode fibers analyzed using impulse response measurements technique," J. Lightwave Technol. **35**(4), 650–657 (2017).
14. C. C. C. Carrero, G. L. Cocq, B. Sévigny, L. Bigot, A. L. Rouge, Y. Quiquempois, M. Bigot-Astruc, D. Molin, and P. Sillard, "Using advanced s2 analysis to measure mode coupling in a 2-lp-mode fiber," in *Optical Fiber Communication Conference*, (Optical Society of America, 2016), p. W4F.5.
15. M. Nakazawa, M. Yoshida, and T. Hirooka, "Measurement of mode coupling distribution along a few-mode fiber using a synchronous multi-channel otdr," Opt. Express **22**(25), 31299–31309 (2014).
16. A. Li, Y. Wang, Q. Hu, D. Che, X. Chen, and W. Shieh, "Measurement of distributed mode coupling in a few-mode fiber using a reconfigurable brillouin otdr," Opt. Lett. **39**(22), 6418–6421 (2014).
17. F. Liu, G. Hu, C. Song, W. Chen, C. Chen, and J. Chen, "Simultaneous measurement of mode dependent loss and mode coupling in few mode fibers by analyzing the rayleigh backscattering amplitudes," Appl. Opt. **57**(30), 8894–8902 (2018).
18. D. Yu, S. Fu, Z. Cao, M. Tang, D. Liu, I. Giles, T. Koonen, and C. Okonkwo, "Mode-dependent characterization of photonic lanterns," Opt. Lett. **41**(10), 2302–2305 (2016).
19. G. Rademacher, R. Ryf, N. K. Fontaine, H. Chen, B. J. Puttnam, R. S. Luis, Y. Awaji, H. Furukawa, and N. Wada, "Channel dynamics in few-mode fiber transmission under mechanical vibrations," in *2020 Optical Fiber Communications Conference and Exhibition (OFC)*, (2020), pp. 1–3.
20. K. Choutagunta, R. Ryf, N. Fontaine, S. Wittek, J. C. Alvarado-Zacarias, M. Mazur, H. Chen, R.-J. Essiambre, R. Amezcua-Correa, T. Hayashi, Y. Tamura, T. Hasegawa, T. Taru, and J. M. Kahn, "Modal dynamics in spatially multiplexed links," in *Optical Fiber Communication Conference (OFC) 2019*, (Optical Society of America, 2019), p. W4C.1.
21. B. J. Puttnam, G. Rademacher, R. S. Luis, H. Furukawa, A. Ross-Adams, S. Gross, M. Withford, N. Riesen, Y. Sasaki, K. Saitoh, K. Aikawa, Y. Awaji, and N. Wada, "Dynamic crosstalk study in a few-mode-multi-core fiber," in *2019 Optical Fiber Communications Conference and Exhibition (OFC)*, (2019), pp. 1–3.
22. J. Fang, G. Milione, J. Stone, G. Peng, M.-J. Li, E. Ip, Y. Li, Y.-K. Huang, P. N. Ji, M.-F. Huang, S. Murakami, W. Shieh, and T. Wang, "Distributed temperature and strain sensing using brillouin optical time-domain reflectometry over a few-mode elliptical-core optical fiber," in *26th International Conference on Optical Fiber Sensors*, (Optical Society of America, 2018), p. TuD1.
23. N. Wang, J. C. Alvarado-Zacarias, M. S. Habib, H. Wen, J. E. Antonio-Lopez, P. Sillard, A. Amezcua-Correa, A. Schülzgen, R. Amezcua-Correa, and G. Li, "Mode-selective few-mode brillouin fiber lasers based on intramodal and intermodal sbs," Opt. Lett. **45**(8), 2323–2326 (2020).
24. H. Wen, H. Zheng, Q. Mo, A. M. Velázquez-Benítez, C. Xia, B. Huang, H. Liu, H. Yu, P. Sillard, J. E. A. Lopez, R. A. Correa, and G. Li, "Few-mode fibre-optic microwave photonic links," Light: Sci. Appl. **6**(8), e17021 (2017).

OSA CONTINUUM

25. G. Rademacher, R. S. Luís, B. J. Puttnam, Y. Awaji, M. Suzuki, T. Hasegawa, H. Furukawa, and N. Wada, "Wideband intermodal nonlinear signal processing with a highly nonlinear few-mode fiber," IEEE J. Sel. Top. Quantum Electron. **26**(4), 1–7 (2020).
26. N. K. Fontaine, R. Ryf, J. Bland-Hawthorn, and S. G. Leon-Saval, "Geometric requirements for photonic lanterns in space division multiplexing," Opt. Express **20**(24), 27123–27132 (2012).
27. S. G. Leon-Saval, N. K. Fontaine, J. R. Salazar-Gil, B. Ercan, R. Ryf, and J. Bland-Hawthorn, "Mode-selective photonic lanterns for space-division multiplexing," Opt. Express **22**(1), 1036–1044 (2014).
28. F. M. Ferreira, C. S. Costa, S. Sygletos, and A. D. Ellis, "Semi-analytical modelling of linear mode coupling in few-mode fibers," J. Lightwave Technol. **35**(18), 4011–4022 (2017).
29. M. Faucher and Y. K. Lize, "Mode field adaptation for high power fiber lasers," in *2007 Conference on Lasers and Electro-Optics (CLEO)*, (2007), pp. 1–2.
30. K. Ho and J. M. Kahn, "Linear propagation effects in mode-division multiplexing systems," J. Lightwave Technol. **32**(4), 614–628 (2014).
31. A. Ellis and N. Doran, "Are few-mode fibres a practical solution to the capacity crunch?" in *2013 15th International Conference on Transparent Optical Networks (ICTON)*, (2013), pp. 1–4.
32. J. Zhou and G. Zheng, "Null space method for tap value initialization in constant modulus algorithm for mode division multiplexing systems," Opt. Express **26**(11), 14552–14566 (2018).
33. Y. Zhao, Y. Liu, C. Zhang, L. Zhang, G. Zheng, C. Mou, J. Wen, and T. Wang, "All-fiber mode converter based on long-period fiber gratings written in few-mode fiber," Opt. Lett. **42**(22), 4708–4711 (2017).
34. B. Li, X. Zhan, M. Tang, L. Gan, L. Shen, L. Huo, S. Fu, W. Tong, and D. Liu, "Long-period fiber gratings inscribed in few-mode fibers for discriminative determination," Opt. Express **27**(19), 26307–26316 (2019).
35. I. Giles, A. Obeysekara, R. Chen, D. Giles, F. Poletti, and D. Richardson, "Fiber lpg mode converters and mode selection technique for multimode sdm," IEEE Photonics Technol. Lett. **24**(21), 1922–1925 (2012).